World Journal of Advanced Research and Reviews
eISSN: 2581-9615 CODEN (USA): WJARAI
Cross Ref DOI: 10.30574/wjarr
Journal homepage: https://wjarr.com/

(RESEARCH ARTICLE)

Check for updates

Design and simulation of a security and surveillance unmanned aerial vehicle

Hakeem SANUSI [1,*], John B. OLADOSU [1], Abdulahi Akintayo TAIWO [1], Faruk Abolore INAOLAJI [1], Olaoluwa John ADELEKE [2], Chukwuemeka Nzeanorue CHRISTIAN [3], Ayanwunmi Olanrewaju SAMUEL[4], Victor Elaigwu ABAH [5] and Deji Ekunseitan KEHINDE [6]

[1] *Department of Computer Engineering, Ladoke Akintola University of Technology, Ogbomoso Oyo State, Nigeria.*
[2] *Department of Electrical Engineering, The Polytechnic Ibadan, Oyo State, Nigeria.*
[3] *Department of Electrical Engineering, George Washington University, Washington Dc, District of Columbia, USA.*
[4] *Department of Electrical Engineering, Yaba College of Technology, Lagos State, Nigeria.*
[5] *Department of Petroleum Engineering, Petroleum Training Institute, Delta State, Nigeria.*
[6] *Department of Industrial Engineering, University of Ibadan, Oyo State, Nigeria.*

World Journal of Advanced Research and Reviews, 2024, 22(03), 148–171

Publication history: Received on 23 April 2024 revised on 02 June 2024; accepted on 04 June 2024

Article DOI: https://doi.org/10.30574/wjarr.2024.22.3.1683

Abstract

The design and simulation of unmanned aerial vehicles (UAVs) have gained significant attention due to their diverse applications in various fields, including surveillance, reconnaissance, environmental monitoring, disaster response, and logistics, this kind of activity suggest that human officers or individual personnel will be able to monitor remotely, live streaming and acquiring specific data from the aerial vehicle while planning or evaluating their operations.

In addition, UAV simulations extend to flight dynamics and control systems, where mathematical models and algorithms are developed to mimic real-world behaviors. These simulations enable the assessment of flight performance, and responsiveness, aiding in the development of control strategies. Simulation plays a pivotal role in refining the UAV design before physical fabrication and testing.

Plotting in MATLAB R2023A 2016a software was used to create detailed 3D models of the UAV and the 6 degrees of freedom in a signal form, with the specifications of maximum roll angle 50^0, pitch angle 30^0, and tilt angle 35^0, which enabling precise visualization and manipulation of components. Aerodynamic simulations, often conducted using computational fluid dynamics (CFD), provide insights into the aircraft's flight characteristics, stability, and control. Structural analysis simulations evaluate the integrity of the airframe under various load conditions.

The simulation shows a very stable operation through an interdisciplinary approach and state-of-the-art simulation tools. The UAV's performance, stability, and safety were evaluated, allowing for iterative refinements in the design. The presented methodology serves as a valuable foundation for the development of cutting-edge UAV technologies that can thrive in diverse operational scenarios.

Keywords: Unmanned aerial vehicles (UAVs); Computational fluid dynamics (CFD); Aerodynamic simulations; Six degrees of freedom (6-DOF); Performance evaluation.

1. Introduction

The continued increase of the world population and its need for protection as well as maintenance of properties has led to the necessity of making great changes in security. The progression in communication, networking, and sensing technologies has involved researchers and investors to deploy a mini-drone which is generally known as Unmanned Aerial Vehicle (UAVs) or Unmanned Aircraft System (Deschênes, 2019).

* Corresponding author: Hakeem SANUSI

A drone is a flying robot that can be controlled remotely or fly autonomously using a software-controlled flight plan in its embedded system that works in conjunction with onboard sensors and a Global Positioning System (GPS). Surveillance is the monitoring of the behavior, activities, or other changing information, usually of people to influence, manage, protect, or direct them. It can survey an area where human intervention is applicable and not applicable (Brener, et al., 2013).

Utilizing a drone for surveillance offers the capacity to perform various functions and grants access to areas that may be challenging or unattainable for humans on foot or in a land vehicle, such as regions with extremely high temperatures or at high altitudes. This includes applications in police investigations across multiple industries as well as rescue missions, among others. A drone is equipped with motors that provide thrust to lift the craft. A drone with four propellers is specifically referred to as a Quadcopter. The fundamental concept underlying the quadcopter is that two motors rotate in a clockwise direction, while the other two revolve in an anticlockwise manner. This allows the aircraft to ascend vertically while utilizing a camera for live streaming and capturing images. (Pawar, et al., 2019).

An Unmanned Aerial Vehicle (UAV) is capable of maintaining controlled and sustained flight, and it is propelled by either a jet, reciprocating, or electric engine. Despite being a relatively recent idea, the origin of UAVs can be traced back to a time before aviation. The early use of UAVs was for surveillance and combat (Akinnuli, et al., 2017). Aerial surveillance has consistently been a crucial aspect of military intelligence. During the onset of World War I, aeroplanes were initially employed as artillery spotter planes, marking the first military application of these vehicles (Kindervater, 2016). Advanced and costly satellite technologies have made surveillance safer and more effective. With recent technological improvements, the UAV has become a vital asset for numerous military organizations worldwide.

The amount of military personnel lost in direct combat has decreased as a result of technology replacing human soldiers. Unmanned aerial vehicles, or UAVs, are employed in a variety of civil and quasi-civil industries in addition to military missions. They include traffic intelligence, environmental protection, disaster management, remote sensing, marine patrol, drug law enforcement, protection of high-value facilities, border control for civil unrest, police surveillance, traffic intelligence, geophysical surveys for oil, gas, and mineral exploration and production, sports, filmmaking for motion pictures, radio message relaying, and weather monitoring. Many tasks have been performed, such as determining various wing design parameters (Sadraey, M and Müller, D. 2009). Aerodynamics for Naval Aviators, written by Etkin and Reid in 1996, concentrated on the fundamental aerodynamic elements that influence every aircraft's performance. Akinnuli et al. (2017) examined several application-relevant polymer and composite material categories.

1.1. Statement of Problem

Unmanned Aerial Vehicles (UAVs) have been very active in recent decades, because of the rapid advancement in design and deployment, so one of the major drawbacks of UAVs is their high energy consumption when it is being deployed, the matter becomes worse during windy weather. The power consumption can be reduced by improving the designs of the UAV and its propeller to increase the overall thrust and the ability of the UAV to be able to understand the particular area to be inspected, ensure complete coverage, and accurate recon reconstruction of the inspected area. The problem of being unable to lift anything but the lightest packages, also the problem of being stolen or vandalized by persons on the ground. The aim of this project is to design and simulate a security and surveillance unmanned aerial vehicle and the specific objectives of the project are To design and simulate a security and surveillance unmanned aerial vehicle using MATLAB R2023A, To develop a detailed design blueprint for the security UAV, considering factors such as size, weight, power, and payload capacity, To test the prototype developed in (ii) in a complex and dynamic environment.

Unmanned Aerial vehicle was simulated using MATLAB R2023A Software alongside the embedded unmanned aerial vehicle toolbox which provides tools and reference application for designing, simulating, testing, and deploying unmanned aerial vehicle, and drone application, e.g. flight log analyzer application that allows one to interactively analyze 3D flight paths, telemetry information and sensor readings from common flight log formats.

The significance of this project lies in its versatility and wide-ranging applications across multiple fields, including observation, surveillance, tactical planning, emergency response, environmental monitoring, security, infrastructure inspection, mapping, surveying, and traffic control in industries such as oil and gas, seaports, and more.

2. Literature review

2.1. Historical and Technological Background

According to defence experts, the development of inexpensive unmanned aerial vehicles (UAVs) may eventually lead to the replacement of advanced manned military aircraft. This development has been seen as a way to reduce the amount of time that personnel are exposed to risk during military operations. Using unmanned aerial vehicles (UAVs) in dangerous places where manned aircraft are at a high risk of being denied access is a cost-effective solution (Hildmann and Kovacs 2019). UAVs, being unmanned and without a crew, have limited range and endurance, thus reducing the chance of loss of human life. An unmanned system (US) or UV is an electromechanical system that operates without a human operator on board. Unmanned vehicles can be operated either through remote control or autonomously, depending on pre-programmed algorithms. A UV/US device is utilized in various contexts due to developments in safety measures.

As the range of applications for drones expands, there are advantages such as enhanced mission safety and reduced operational expenses (Zhuo, et al., 2017). There are three distinct classifications of unmanned vehicles or systems. Which include: Unmanned or Autonomous Aerial Vehicle (UAV/AAV) (Demir, et al., 2015), Unmanned or Autonomous Ground Vehicle (UGV/AGV) (Fernandez, et al., 2019) and Unmanned/Autonomous Underwater Vehicle (UUV/AUV) (Jain, et al., 2015).

Unlike UAVs, other UV classes lack widespread adoption. Over the past few years, there has been a rapid and continuous advancement in technology related to Unmanned Aerial Vehicles (UAVs). UAVs, commonly referred to as drones (Dynamic Remotely Operated Navigation Equipment), are the predominant type of unmanned aircraft systems in the United States.

An unmanned aerial vehicle (UAV) has the capability to navigate through the atmosphere, conduct surveillance over vast regions, and access environments that are dangerous for humans. Moreover, UAVs are becoming more autonomous in their operations. Unmanned Aerial Vehicles (UAVs) have the capability to carry out many tasks, including automatic take-off, landing, obstacle detection and avoidance, as well as course mapping (Oubbati, et al., 2019). A drone is a unique aircraft that combines innovative robotics, aeronautics, and electrical components. Drones offer a viable alternative to satellites for acquiring information in a faster and more cost-effective manner (Alzahrani, et al., 2020). Unmanned aerial vehicles possess the capability to shoot exceptional aerial images and films, as well as gather extensive and accurate data, thanks to their high-quality cameras coupled with advanced sensors. Drones serve as reliable and easily noticeable providers of public services in various fields, including surveillance, transportation, farming, and disaster management. The terms "unmanned aerial vehicle" and "drone" are used interchangeably in this project.

2.2. Control Strategy of a Quadcopter

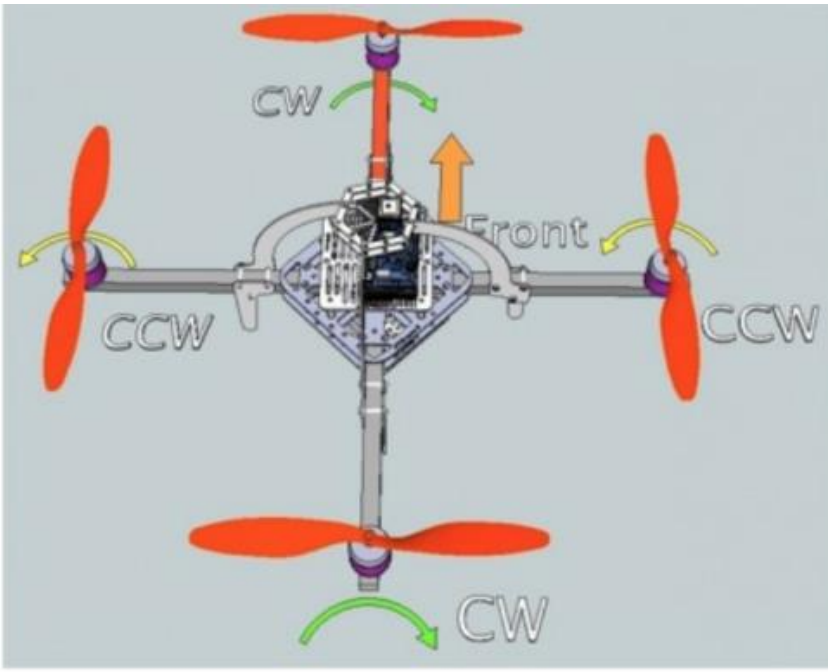

Figure 1 How Quadcopter Propellers Operate. (Stafford, 2014).

The control strategy of a quadcopter involves a combination of hardware components, sensors, and software algorithms working together to stabilize and control the aircraft's motion. Quadcopters, being multirotor aircraft with four rotors, require precise control to maintain stability and achieve desired flight characteristics (Hoffmann, et al., 2007).

Figure 2.1 shows the control strategy of a quadcopter Two of the rotors spinning clockwise (CW) and the other two rotors spin counterclockwise (CCW). Flight control is provided by independent variation of the speed and hence lift and torque of each rotor. Pitch and roll are controlled by varying the net centre of thrust, with yaw controlled by varying the net torque (Stafford, 2014).

A sensor converts the physical action to be measured into an electrical equivalent and processes it so that the electrical signals can be easily sent and further processed. The sensor can output whether an object is present or not present (binary) or what measurement value has been reached (analog or digital). Here's a general overview of the control strategy for a quadcopter

2.2.1. Ultrasonic Sensor

Ultrasonic sensors are instruments that generate sound waves and calculate the duration it takes for the waves to reflect off objects and come back to the sensor. Subsequently, this data is utilized to compute the distance separating the drone from the object. By utilizing this data, unmanned aerial vehicles can identify barriers in their trajectory and adapt their flying trajectory accordingly. This enables them to prevent collisions and mitigate other potential dangers. In addition, ultrasonic sensors can be utilized to gauge the drone's altitude, enabling it to sustain a steady height relative to the ground. Ultrasonic sensors have the capability to assist drones in both navigation and wind detection. By detecting wind speed and direction, drones can make necessary adjustments to their flight route in order to avoid encountering high winds.

2.2.2. Camera

A camera takes in images at 60 frames per second using image processing techniques called optical flow. Optical flow is a technique used to describe image motion. It is usually applied to a series of images that have a small time step between them, for example, video frames. Optical flow calculates a velocity for points within the images, and provides an estimation of where points could be in the next image sequence.

2.2.3. Pressure Sensor

Drones utilize air pressure sensors to stabilize altitude, allowing hover capabilities needed for videography or photography. Combined with the accelerometer and gyroscope, barometric pressure sensors enable drones to fly with precision. As a barometer measures changes in altitude, a pressure sensor can rapidly measure changes in atmospheric pressure to help ensure the UAV is flying at the appropriate elevation.

2.2.4. Inertial Measurement Unit Sensor

Inertial measurement units combined with GPS are critical for maintaining direction and flight paths. As drones become more autonomous, these are essential to maintain adherence to flight rules and air traffic control. IMUs are used for a variety of applications in UAVs and drones. They allow the aircraft to maintain stability and control while experiencing high winds or performing steep turning maneuvers. They can also be used to enable highly accurate station-keeping or autonomous waypoint.

2.3. Quadcopter material

2.3.1. Frame

This is the most important basic part of quadcopter, as the name indicates, as shows in Figure 2.2 the copter has 4 arms, the frame should be light as well as rigid to host LIPO battery, 4 BLDC motors, 4 ESC and controller.

Aluminium or wood channel can be used to build frames, but the F45 frame's arms are composed of an ultra-strength material that can withstand any impact, and the frame boards are made of a high-strength compound PCB, which simplifies and makes wiring batteries and ECSs safer. Selecting the ideal frame for quadcopters is the first step in designing a quadcopter.

Figure 2 A Frame (Ahmed, et al., 2021)

2.3.2. DC Brushless motor

Figure 2.3 shows a brushless DC motor which is an internally communicated electric motor designed to be run from a direct current power source. Brushed motors were the first commercial.

Figure 3 A Brushless DC Motor (Ahmed, et al., 2021)

For over a century, DC distribution systems were utilized to power motors in commercial and industrial structures, marking a significant advancement in the usage of electric power for moving mechanical energy. The operating voltage and magnetic field strength can be adjusted to vary the speed of brushed DC motors. A brushed motor's speed and torque characteristics can be changed to produce a continuous speed that is inversely proportional to the mechanical load, depending on how the field is connected to the power supply. Cranes, paper machines, steel rolling mills, and electrical propulsion all still employ brushed motors. Brushless DC motors that use power electronic devices have replaced brushed motors in many applications since brushes wear out and need to be replaced.

One side of the positive pole experiences an upward push while the other side experiences a downward force when current flows through the coil wound around a soft iron core. Fleming's left-hand rule states that the forces turn the

coil, causing it to rotate. A "direct current" commutator causes the current to reverse direction every half a cycle (in the case of a two-pole motor) in order to keep the motor rotating in the same direction.

2.3.3. Electronic Speed Control ESC

Drone flight controls can regulate and alter the speed of the aircraft's electric motors with the use of electronic speed controllers, or ESCs. As seen in Figure 2.4, an instruction from the flight controller triggers the ESC to adjust the voltage to the motor, which in turn modifies the propeller's speed.

The amount of power supplied by the battery to the ESC fluctuates in response to the input signal. ESC is equipped with a battery elimination circuit (BEC). The 5V output of the ESC that powers the receiver, servo motor (for the camera gimbal), and FC is all that BEC consists of. An ESC may be an independent component that connects to the throttle control channel of the receiver, or it may be integrated into the receiver, as is the case with the majority of toy-grade RC vehicles. Certain remote control (RC) manufacturers incorporate hobby-grade electronics into their entry-level aircraft, vessels, or vehicles via on-board electronics that integrate both components onto a single circuit board.

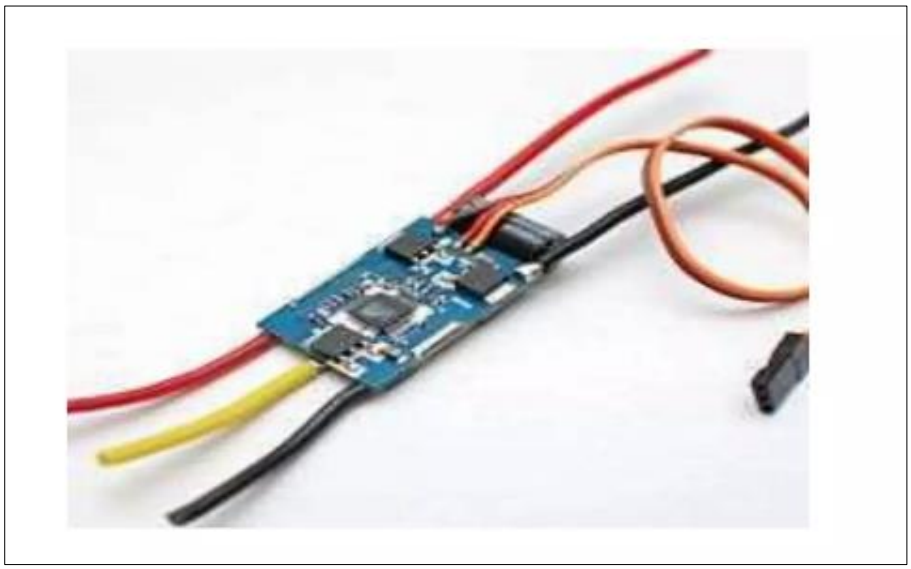

Figure 4 Electronic Speed Control (Ahmed, et al., 2021)

Generic ESC modules with a 35 ampere current rating and an integrated BEC are not compatible with brushless motors. This is because brushless motors and brushed ESC systems differ fundamentally. Brushes ESC systems use an on-board DC power input to provide a limited-voltage, tri-phase AC power output that powers brushless motors by a sequence of AC signals produced by the ESC's electronics and an extremely low rotational impedance. Brushless motors, also called "out runners" or "in runners" depending on how they are put together physically, have become quite popular among fans of "electro flight" radio-control aero modelling. This is because, in comparison to traditional brushed motors, brushless motors have higher efficiency, power, durability, and low weight. Brushless AC motor controllers, on the other hand, have far more complicated designs than their brushed counterparts.

2.3.4. Propeller

Propellers are devices that transform rotary motion into linear thrust as shows in Figure 2.4. Drone propellers provide lift for the aircraft by spinning and creating an airflow, which results in a pressure difference between the top and bottom surfaces of the propeller. The drone propeller is like the fan of the drone, It's the blade that spins and creates lift and thrust. It's usually mounted on the motors of the drone and spins really fast thanks to the motor's rotation. It's like the wing of a bird, it's what makes the drone fly.

Typically expressed in inches, Props must be smaller as the Kv of the motor increases. Although smaller props enable higher velocities, they do so at the expense of reduced efficiency.

Figure 5 Propeller (Ahmed, et al., 2021)

2.3.5. LI-PO Battery

A lithium polymer battery, or more precisely, lithium polymer battery (abbreviated LiPo, LIP, Li-poly, and others), is a lithium-ion rechargeable battery that operates on a polymer electrolyte rather than the more prevalent liquid electrolyte. The electrolyte for lithium-ion (LiPo) cells produces semisolid (gel) polymers with high conductivity; these are utilised in tablet computers and numerous cellular telephone handsets.

In addition to the ESC motors, the battery that powers the quadcopter must supply power to all onboard sensors, processors, and motors. Without overheating, the battery must supply power to the apparatus for a minimum of six minutes. Additionally, the battery must be equipped with protective circuitry to avert overcharging and overdischarging, both of which have the potential to ignite and detonate batteries..

Lithium Polymer LIPO rechargeable batteries have exploded in popularity among electric RC enthusiasts, particularly quadcopters. They are the primary reason why fuel-powered aircraft are no longer a viable alternative to electric aircraft. LiPo batteries are incredibly powerful despite their diminutive size. They have sufficient discharge rates to supply power to quadcopters. Bear in mind that lithium-ion batteries are considerably costlier and can only withstand 300 to 400 charge cycles. The LiPo must be charged, discharged, and stored with particular care. LiPo contain a volatile electrolyte that, if mismanaged, can easily cause rupture or ignition. LiPo battery cells have a rated voltage of 3.7 volts per cell, as opposed to the 1.2 volts per cell of conventional NiCad battery cells.

Figure 6 Battey (Ahmed, et al., 2021)

2.3.6. Remote Control

Figure 7 Remote Control (Trilaksono, et al., 2013).

An RC Transmitter (2.4GHz RC radio transmitter) for controlling the position and direction of the quadcopter. The quadcopter receives commands from the RC transmitter on the ground via a 2.4GHz RC radio receiver. (Link in only one direction). Handheld controllers serve as transmitters, enabling remote control of the craft. It is equipped with a number of switches, two sticks, two trim controls (or sliders per stick), a display, and a power button. In order for transmitters and receivers to function, they require a specific frequency range. Utilizing digital spectrum modulation, the new frequency range is 2.4GHz. The ISM (Industrial Scientific and Medical) Radion band operates without a license at 2.4GHz. Nevertheless, a specific rod movement corresponds to a particular aircraft motion determination mode. Of the four transmitter modes, mode 2 is the most prevalent and is typically the default setting on the majority of radios.

2.3.7. Receiver

Figure 8 Receiver (Trilaksono, et al., 2013).

A radio receiver is an apparatus that is able to receive directives from a radio transmitter and convert them into specific actions for aircraft control via interpretation by the flight controller. The protocol for radio communication can be divided into two groups:

- Tx Protocols between Radio Transmitter and Radio Receiver
- Rx Protocols between Radion Receiver and Flight Controller.
- Tx Protocols are in most cases specific to brands
- FrSky: D8, D16, LR12
- Spektrum: DSM, DSM2, DSMX
- FlySky: AFHDS, AFHDS 2A
- Futaba: FASST
- Hitec: A-FHSS
- Devo: Hi-Sky

As for Rx Protocols, some of them are universal

PCM, PWM, PPM, SBUS

2.4. Application Unmanned Aerial Vehicle

2.4.1. Security, Monitoring and Surveillance

UAVs are indispensable to military surveillance operations. Multiple nations have incorporated UAVs into their strategic defence plans. Flying robotics machines are being employed by nations for anti-poaching operations, adversary detection, maritime monitoring of vital sea lanes, and border control. Presently, unmanned aerial vehicles (UAVs) that are economical, dependable, and adaptable are making a substantial impact in the realm of aerial surveillance, monitoring, and surveying with the aim of averting illicit operations. For instance, surveillance for any hazard and monitoring of movement activity in any restricted area can be accomplished with the aid of drones. UAVs are capable of delivering these services through the detection of an automated alert system that requires minimal manual intervention.

2.4.2. Disaster Management

When confronted with man-made or natural catastrophes, such as tsunamis, floods, or terrorist attacks, UAVs have the capability to access disaster vehicle locations that are perilous for human habitation. The infrastructure of telecommunications, transportation, power, and water utilities may be severely damaged by these catastrophes. UAVs can assist with information gathering, detritus navigation, and the need for prompt solutions. The utilization of UAVs equipped with radars, sensors, and high-quality cameras can aid rescue teams in the detection of damage, enabling them to commence recovery operations and dispatch resources like manned helicopters and first aid supplies without delay. UAVs can aid in the estimation of disasters in a timely manner, deliver disaster notifications, and aid in the development of effective countermeasures. A swarm of fire extinguisher-equipped drones can monitor, inspect, and trace any area in the event of a wildfire without jeopardizing human lives. Thus, unmanned aerial vehicles (UAVs) can aid in the coverage of expansive areas in real-time while ensuring the security and welfare of personnel present. Early warning capabilities of unmanned aerial vehicles (UAVs) can aid in the rescue of endangered humans and fauna.

2.4.3. Remote Sensing

High-resolution imagery data of remote regions, islands, summits, and coastlines is presently obtained via amateur drone technology. UAV technology connects remote sensing data collected from the earth, space, and aircraft. Ultra-lightweight and low-cost UAVs enable the execution of high-quality observations with precise temporal and spatial resolutions. Disease detection, water quality monitoring, drought monitoring, oil and gas, yield estimation, hydrological modeling, biodiversity conservation, geological disaster survey, terrain survey, forest mapping, and crop monitoring are all applications that can be aided by the remote sensing capabilities of unmanned aerial vehicles (UAVs). In addition to crowdsourced mapping and the construction of three-dimensional environmental maps, this technology has found application in the fields of archaeology and cartography. Deviling at a reasonable cost can furnish land planning with up-to-date information that does not require reliance on obsolete cartography sources.

2.4.4. Search and Rescue SAR

UAVs play a crucial role in numerous critical situations, including but not limited to disaster management, rescue operations, and public safety. By providing real-time imagery data of target locations, UAVs can aid in the conservation of manpower, resources, and time. As a result, a SAR team is capable of promptly identifying and selecting the precise location where immediate assistance is needed. When confronted with catastrophic situations such as missing persons, avalanches, wildfires, or noxious gas infiltration, UAVs can expedite SAR operations. Drones may be utilized, for instance, to locate and reunite missing mountaineers or to safeguard human lives in remote deserts and forests. Drones

have the capability to aid in the tracing of unfortunate victims, traversing difficult terrains, and navigating adverse atmospheric conditions. Medical supplies can be delivered by drones prior to the arrival of an ambulance or medical squad. Provisions of food, medical equipment, and life-saving jackets can be loaded onto drones for delivery to remote locations and disaster-stricken regions. Stashed individuals in inaccessible regions may receive provisions such as clothing, water, and other essential items from these drones prior to the advent of rescue crews.

2.4.5. Construction and Infrastructure Inspection

The utilization of UAVs has simplified, expedited, and optimized as-built mapping, construction monitoring, and site inspection. Site work progress is maintained at a high standard when construction projects are monitored from beginning to end. It is capable of furnishing potential stakeholders with reports that encompass imagery, video, and 3D mapping. Infrastructure and construction inspection applications can be substantially aided by this technology. A growing interest is being observed in the utilization of unmanned aerial vehicles (UAVs) for monitoring construction projects, gas pipelines, GSM antennas, and power lines. Shakhatreh et al. (2019) state the following.

2.4.6. Real-Time Monitoring of Road Traffic

Unmanned aerial vehicles (UAVs) have garnered a lot of interest in the field of road traffic monitoring (RTM) systems. Menouar et al. (2017) claim that RTM can totally automate the transportation industry with the usage of UAVs. This will include automating field support teams, traffic cops, road surveyors, and rescue squads. The automation of these components can be aided by intelligent and dependable UAVs. UAVs are becoming a viable option for gathering information regarding traffic conditions on roadways. Drones that are affordable can monitor vast road segments, as opposed to traditional monitoring tools like loop detectors, microwave sensors, and security cameras (Shakhatreh et al., 2019). Local law enforcement agencies can use drones to gain a clear view of traffic accidents or to conduct a thorough security operation against highway crimes like auto theft. Additional uses include tracking down armed robbers, hijackers, and traffic infractions, as well as identifying automobiles and conducting raids on suspicious vehicles. In addition, it can help prevent traffic jams and mass congestion by detecting overspeeding vehicles and accidents. (Elloumi and others, 2018).

2.5. Related Works

UAV-based solutions have grown significantly over the previous ten years, especially in the last five years. NASA experts outlined a wide range of civil uses for unmanned aerial vehicles (UAVs) in 2004 (Cox et al.), highlighting the technology's impending potential in areas such as land management, national security, Earth sciences, and business. Years later, this tentative study was confirmed by authors like Hugenholtz et al. (2012), who detailed how the usage of UAVs may revolutionise research methodologies in the disciplines of Earth sciences and remote sensing. The results of a comprehensive study into the many aspects of unmanned aerial vehicles (UAVs) are presented by Abdel-Aziz et al. (2015). These findings highlight the potential applications of UAVs in photogrammetry, forestry, agriculture, disaster relief, localization and rescue, surveillance, environmental monitoring, and vegetation monitoring, among other domains.

In reviewing studies that use quadrotor multicopters, researchers like Colomina and Molina (2014), claim that because of their small size, manoeuvrability, and ease of use, these devices are used in a variety of domains, including Earth Sciences, national security, civil engineering, search and rescue, emergency response, military surveillance, border patrol, and surveillance. We are more interested in atmospheric sampling as it relates to the measurement of air pollution. In this specific research topic, Anderson and Gaston highlight how unmanned aerial vehicles (UAVs) are appropriate for ecological reasons. They highlight the recurrent problem that data obtained with conventional methods' geographical and temporal resolutions are insufficient to meet the requirements of locally focused ecological research. Additionally, the use of unmanned aerial vehicles (UAVs) at low altitudes and speeds opens up new possibilities for monitoring biological phenomena by enabling the transfer of data with improved spatial resolution.

Hildmann and Kovacs (2019) explain how photos taken by small unmanned aerial vehicles (UAVs) are gradually replacing the far more expensive high-definition satellite imagery that is used to analyze changes in crop and soil conditions. Unmanned aerial vehicles (UAVs) in particular are thought to be a good alternative to traditional environmental monitoring techniques because of their affordable operation, excellent spatial and temporal resolution, and flexible scheduling of image captures. A prime example of the study shows how a multicopper fitted with a thermal camera could be utilized to obtain an extremely precise representation of the water levels in a vineyard, thereby advancing the field of precision agriculture. In reference to the research topic, while a great deal of literature has been written about the use of Unmanned Aerial Systems (UAS) for explosive detection, most of these articles focus on the formation of swarms or the information sharing between them. The mobility model put forth by Zhou et al. (2004),

which depicts a group of nodes moving over "Virtual Tracks" (highways, valleys, etc.) in a predefined "Switch Station" mode, is an example of such research. Nodes can split off or combine with another group of nodes on these tracks. Extensive research has been carried out with sensor attachment in unmanned aerial vehicles.

Erman et al. (2008) used an unmanned aerial vehicle (UAV) fitted with a sensor to create a wireless sensor network. This permits any UAV to operate as a sink or a node; nevertheless, the authors do not try to optimise the process of monitoring. A fixed-wind aeroplane fitted with a sensor node that serves as a mobile gateway was presented by Teh et al. This aircraft makes it easier for the unmanned aerial vehicle (UAV) to communicate with different stationary base stations that monitor pollution. In this case, the UAV retrieves only the data that the stations collected. A proposal for the creation of a lightweight laser-based sensor that UAVs may use to measure trace gas species was made by Khan et al. (2012) in their paper. The primary focus of the authors' investigation was how the optical sensor gathers samples of air pollution. Illingworth et al. show that the UAV improves the sample granularity by using large-scale aircraft equipped with ozone sensors to automate the coverage of a vast area. Looking over the corpus of work on UAS mobility control models used for air pollution monitoring, it is clear that very little of it is focused on improving coverage in a particular area.

To limit or eliminate the sudden stops and sharp bends that are typical of the random waypoint mobility model, for example, Biomo et al. (2014) presented a mobility model that makes use of the Enhanced Gauss-Markov model. Additionally, Wang et al. (2010) presented a model based on semi-random circular movement (SRCM). A random waypoint mobility model is used to compare the acquired findings in order to evaluate the coverage and network connectivity. Orfanus et al. (2014) conducted a comparative analysis of their algorithms and models that utilized random waypoints, Markov chains, and Brownian motion. Finding out how collision avoidance systems affected the amount of time needed to finish area coverage was the goal. In UAV environments, Kuiper and Nadjm-Tehrani (2006) compared the results of direction decision engines (next waypoint) using the "Random Mobility Model" and the "Distributed Pheromone Repel Mobility Model."

An algorithm for moving over a predetermined area was presented by Wan et al. (2013). After choosing a point in space and a line perpendicular to its bearing direction, the system uses geometric factors to steer the UAV. Implementing UAVs for certain missions that need autonomous mobility is being worked on. The work of Sánchez-García et al. (2015) provides an example of this; they suggest a mobility model for the autonomous deployment of an aerial ad hoc network in the case of a disaster, with the goal of providing victims with a communications infrastructure that is flexible and mobile. The suggested mobility model, which controls how the network's unmanned aerial vehicles are deployed, is based on the Jaccard dissimilarity metric. Similar work is provided, according to Briante et al. (2015), in which an in-network density analysis is used to determine the physical regions that need to be visited by a flying robot. If one only looks at previous mobility model suggestions, academic publications such as Bouachir et al. (2014), who presented the Paparazzi Mobility Model (PPRZM), can be found. The developers of this model identified five different movement types: Stay-On, Waypoint, Eight, Scan, and Oval. These motions followed a predefined state machine and had different odds of changing states. Even the navigational habits of animals have been studied. The study by Basu et al. (2004) provides an example of this kind of research; it looks at UAV placement and navigation strategies in an attempt to enhance network connectivity by utilizing local flocking principles, which are frequently seen in aerial organisms like insects and birds.

3. Methodology

3.1. Vehicle Dynamic

The understanding of 6-degrees of freedom (6-DOF) is crucial for expressing the quadcopter's motion through equations. The 6-DOF concept provides three-dimensional information regarding the position and orientation of a vehicle. The dynamic equations of a vehicle merely depict the position and orientation change that occurs with time. In this instance, I assumed the earth to be flat, the gravitational force to be constant, the centre of mass to be equal to the centre of gravity, and the quadcopter structure to be rigid.

3.1.1. Six-Degrees of Freedom (6-DOF)

Six Degrees of Freedom (6-DOF) refers to the ability of an object or system to move freely in three-dimensional space along six distinct axes. This concept is often used in various fields such as robotics, aerospace engineering, virtual reality, and video games to describe the complete range of motion that an object can have. Each degree of freedom corresponds to a specific axis of rotation or translation, and together, they define the object's spatial orientation and position. Here's the details of each degree of freedom as shows in Figure 3.1.

- Translation along the X-axis: This degree of freedom allows the object to move forward and backward along the X-axis. Positive movement indicates forward motion, and negative movement indicates backward motion.
- Translation along the Y-axis: This degree of freedom enables the object to move left and right along the Y-axis. Positive movement signifies movement to the right, while negative movement signifies movement to the left.
- Translation along the Z-axis: With this degree of freedom, the object can move up and down along the Z-axis. Positive movement corresponds to upward motion, and negative movement corresponds to downward motion.
- Rotation around the X-axis (Roll): This degree of freedom allows the object to rotate around the X-axis. Positive rotation produces a rolling motion, where one end of the object rises while the other end descends.
- Rotation around the Y-axis (Pitch): This degree of freedom enables the object to rotate around the Y-axis. Positive rotation leads to a pitching motion, causing one end of the object to rise while the other end lowers.
- Rotation around the Z-axis (Yaw): This degree of freedom allows the object to rotate around the Z-axis. Positive rotation results in a yawing motion, causing the object to rotate left or right.

In combination, these six degrees of freedom allow an object to achieve a wide range of movements and orientations in space.

3.1.2. Orientation and Frames of References

The precise location of the vehicle can be determined using x, y, and z coordinates, which represent the distances from an inertial frame of reference, which is a fixed point on the earth. Coordinates are typically in the cardinal directions of north, east, and down. The angles φ, θ, and ψ are utilised to denote the orientation or attitude of the vehicle, respectively, in relation to the body frame reference. This reference is a coordinate system whose origin is the body's centre of gravity (Cg). A visual representation of the frames of reference is presented in Figure 3.2 to facilitate comprehension.

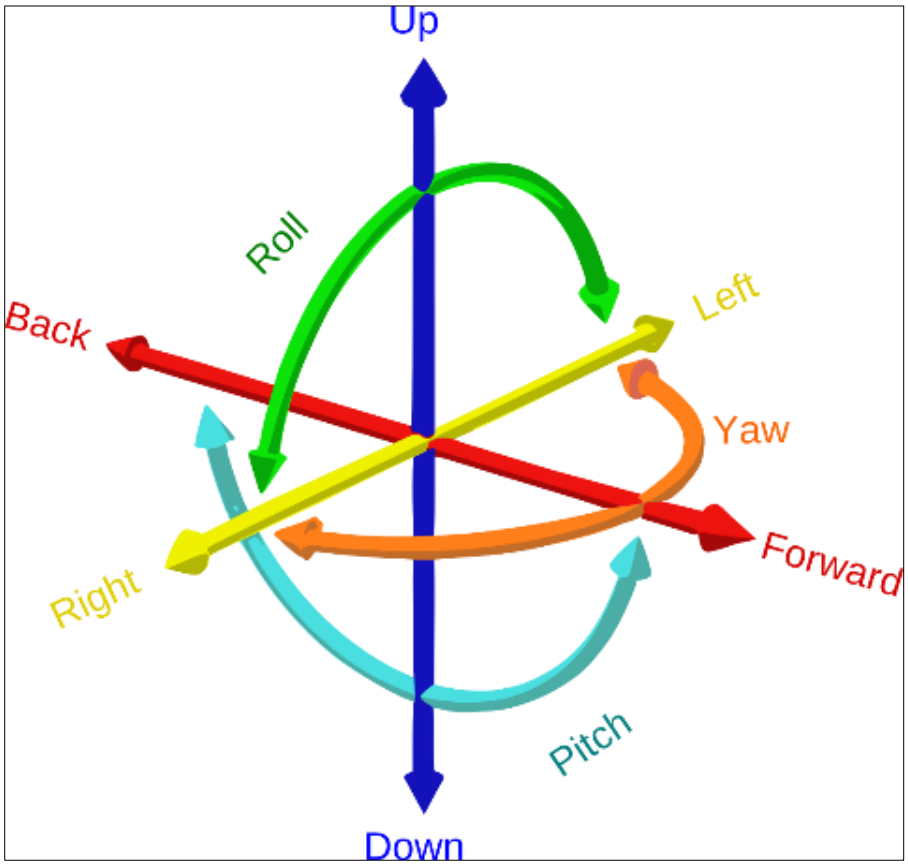

Figure 9 Six-Degrees of Freedom (Wikipedia)

3.2. Euler Angles

The central objective of this research is the attitude control of the quadcopter. The orientation of the vehicle can be determined using various methods, including trigonometric functions, Euler angles, and quatrains. In consideration of simplicity, Euler angles were employed despite the presence of singularity concerns. The determination of the vehicle's

ultimate orientation in relation to the body frame can be achieved by employing an inertial-to-body frame transformation matrix and Euler angles. For vector transformation, matrix multiplication is a practical method. Consider (b1, b2, and b3) to be a body frame of reference, while (x, y, and z) represent an inertial frame of reference. The displacement of the other two body frame axes with respect to the inertial frame axes occurs when an object rotates about one of the body frame axes. Likewise, the axis of rotation maintains a parallel alignment with the axis of inertia that it corresponds to. The axes of a rotated body frame may be denoted by equations for inertial trigonometric functions. In subsequent stages, trigonometric equations may be represented as matrices. In the same manner, two additional matrices can be obtained through the rotation of the remaining two body frame axes. The rotational motion of the three body frame axes b1, b2, and b3 is illustrated in Figure 3.3. The equations and matrix representations of the corresponding inertial trigonometric functions are also presented.

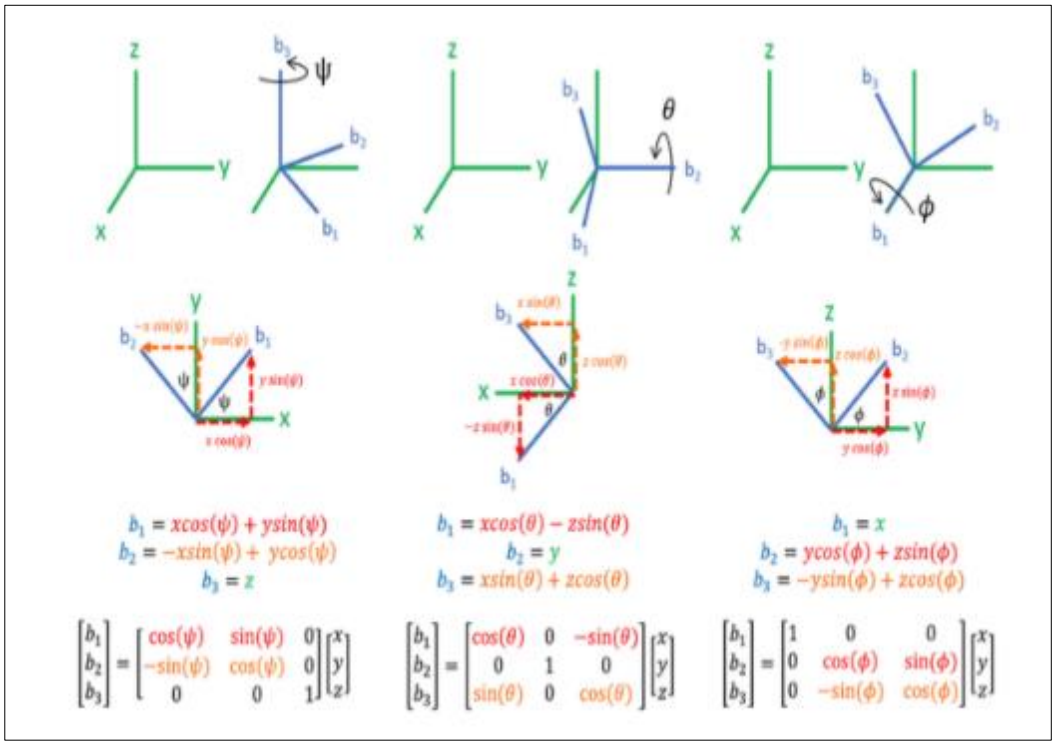

Figure 10 Euler angles

The orderly combination of these three matrices which is shows in Figure 3.3 gives the inertial to body frame transformation matrix. Order of the operations is really important.

$$\begin{bmatrix} b1 \\ b2 \\ b3 \end{bmatrix} = \begin{bmatrix} 1 & 0 & 0 \\ 0 & \cos(\varphi) & \sin(\varphi) \\ 0 & -\sin(\varphi) & \cos(\varphi) \end{bmatrix} \begin{bmatrix} \cos(\theta) & 0 & -\sin(\theta) \\ 0 & 1 & 0 \\ \sin(\theta) & 0 & \cos(\theta) \end{bmatrix} \begin{bmatrix} \cos(\psi) & \sin(\psi) & 0 \\ -\sin(\psi) & \cos(\psi) & 0 \\ 0 & 0 & 1 \end{bmatrix} \begin{bmatrix} x \\ y \\ z \end{bmatrix} \quad 3.1$$

All three matrices representing the trigonometric equations are multiplied to get a single transformation matrix C_n^b shows in equation 3.2 which will be used for inertial-to-body frame transformation.

$$\begin{bmatrix} b1 \\ b2 \\ b3 \end{bmatrix} = \begin{bmatrix} \cos(\theta)\cos(\psi) & \cos(\theta)\sin(\psi) & -\sin(\theta) \\ -\cos(\theta)\sin(\psi) + \cos(\psi)\sin(\varphi)\sin(\theta) & \cos(\psi)\cos(\varphi) + \sin(\theta)\sin(\varphi)\sin(\psi) & \text{coss}(\theta)\sin(\varphi) \\ \sin(\psi)\sin(\varphi) + \sin(\theta)\cos(\varphi)\sin(\psi) & -\sin(\varphi)\cos(\psi) + \sin(\theta)\cos(\varphi)\sin(\psi) & \text{coss}(\theta)\cos(\varphi) \end{bmatrix} \begin{bmatrix} x \\ y \\ z \end{bmatrix} \quad 3.2$$

For the transformation from the body to the inertial frame theoretically the inverse of the transformation matrix C_n^b is used. As transformation matrices are orthonormal, we can simply use the transpose of the transformation matrix $R^t = R^{-1}$.

$$\begin{bmatrix} x \\ y \\ z \end{bmatrix} = \begin{bmatrix} \cos(\theta)\cos(\psi) & -\cos(\theta)\sin(\psi) + \cos(\psi)\sin(\varphi)\sin(\theta) & \sin(\psi)\sin(\varphi) + \sin(\theta)\cos(\varphi)\sin(\psi) \\ \cos(\theta)\sin(\psi) & \cos(\psi)\cos(\varphi) + \sin(\theta)\sin(\varphi)\sin(\psi) & -\sin(\varphi)\cos(\psi) + \sin(\theta)\cos(\varphi)\sin(\psi) \\ -\sin(\theta) & \text{coss}(\theta)\sin(\varphi) & \text{coss}(\theta)\cos(\varphi) \end{bmatrix} \begin{bmatrix} b1 \\ b2 \\ b3 \end{bmatrix} \quad 3.3$$

Equation 3.3 shows the transpose of the equation 3.2 matrix.

Now using equations 3.2 and 3.3, I can find the orientation of the vehicle with respect to the body frame and inertial frame. (Tytler 2017a.)

3.3. Equation of Motion

3.3.1. Variable

The spatial location and orientation of the vehicle are presently established. The equations of motion for the vehicle require the variables from Table 3.1, which contain the quadcopter's linear and angular velocities. The dynamics equations can be derived by employing the right-hand rule and an ancient convention that defines X, Y, and Z as North, East, and Down, respectively.

Table 1 Velocity Linear Variables

V^b	**Linear velocity in the body frame**
U	Longitudinal velocity
V	Lateral velocity
W	Normal velocity

Table 2 Rotational Velocity Variables

W^b	**Rotational velocity in the body frame**
P	Roll rate
Q	Pitch rate
R	Yaw rate

Table 3 Forces

Fx	Force in the X direction
Fy	Force in the Y direction
Fz	Force in the Z direction

Table 4 Euler Angles

Φ	Roll angle
Θ	Pitch angle
Ψ	Yaw angle

Table 5 Moment of Torques

L	A rotational moment along the X-axis
M	A rotational moment along the Y-axis
N	A rotational moment along the Z-axis

3.3.2. Inertial Motion in Body Frame

Due to the presumption that the vehicle body is rigid, the body components with respect to the body structure remain immobile. Since the body is equipped with sensors and propellers, I aim to derive equations of motion using body frame

coordinates that are not dependent on an inertial frame. These equations can subsequently be applied to any inertial starting point. As stated by Tytler (2017b)

3.3.3. The Chain Rule

The chain rule simultaneously provides the mathematical representation of the inertial motion in the body frame. We take the derivative of the inertial frame vectors to represent them in the body frame. The chain rule of derivation can be used to determine the derivatives of the change brought about by the time derivative of the vector inside the coordinate frame and the time derivative of the coordinate frame rotation. Where $\breve{b_1}, \breve{b_2}$ *and* $\breve{b_3}$ in equation 3.4 are unit vectors associated with the body frame to represent the inertial frame velocity in the body frame.

$$V^b = \begin{bmatrix} u \\ v \\ w \end{bmatrix}^b = u\breve{b_1} + u\breve{b_2} + u\breve{b_3} \tag{3.4}$$

Applying the Chain rule to equation 3.4 we get equation 3.5.

$$\left(\frac{dV}{dx}\right)_{inertial} = \left(\frac{du}{dt}\breve{b}_1 + \frac{dv}{dt}\breve{b}_2 + \frac{dw}{dt}\breve{b}_3\right) + \left(u\frac{db_1}{dt} + v\frac{db_2}{dt} + w\frac{db_3}{dt}\right) \tag{3.5}$$

The inertial velocity in the body coordinates is represented by the first set of brackets in equation 3.5 above. The second set shows how coordinate frame rotation affects velocity. The Coriolis Theorem, which is the cross product of angular velocity and a velocity vector indicating frame rotation, allows us to rewrite equation 3.5 above as equation 3.6.

$$\dot{V}_{inertial} = \dot{V}^b + W_n^b * V^b \tag{3.6}$$

Further, it can be represented as a skew-symmetric matrix as shows in equation 3.7.

$$W * v = [w*]v = \begin{bmatrix} 0 & -w_z & w_y \\ w_z & 0 & -w_x \\ -w_y & w_z & 0 \end{bmatrix} V \tag{3.7}$$

3.3.4. Newton's Second Law of Motion

So far, I've learned how to alternate between the body and inertial frames as well as how to create motion in the body frame of reference. Equation 3.8, which expresses Newton's Second Law of Motion, indicates that one can obtain both linear and rotational equations of motion by multiplying the acceleration (a) or the derivative of velocity (v) by the change in momentum (P) or mass (m).

$$F = \frac{dp}{dt} = m\frac{dV}{dt} = ma \tag{3.8}$$

By multiplying Equation 3.8, which gives linear momentum, by a position vector $(\vec{r})$, one can obtain angular momentum, or Equation (3.9).

$$H = (\vec{r}) * F = (\vec{r}) * m\frac{dV}{dt} \tag{3.9}$$

Further simplification of the relationship between moment (M) and change in angular momentum (H) yields the product of angular acceleration (Ω) and moment of inertia (I), where Ω is the derivative of angular velocity (ω) for continuously mass-distributed objects. Equation 3.9 is transformed to produce Equation 3.10. Tytler (2017a),

$$M = \frac{dH}{dt} = I\frac{d\omega}{dt} = I\Omega \tag{3.10}$$

So, I derived linear and rotational equations separately.

3.4. External Forces and Moments

The external forces and moments acting on the vehicle's body are necessary to calculate the translation equations of motion.

3.4.1. Thrust

While the thrust produced by the quadcopter's propellers operates perpendicular to the vehicle, the moment functions at the centre of gravity of the vehicle. Figure 3.4 shows the separation between the propellers and the centre of gravity (CG) of the vehicle. These lengths are then factored into the computation of the moment around the vehicle's centre of gravity.

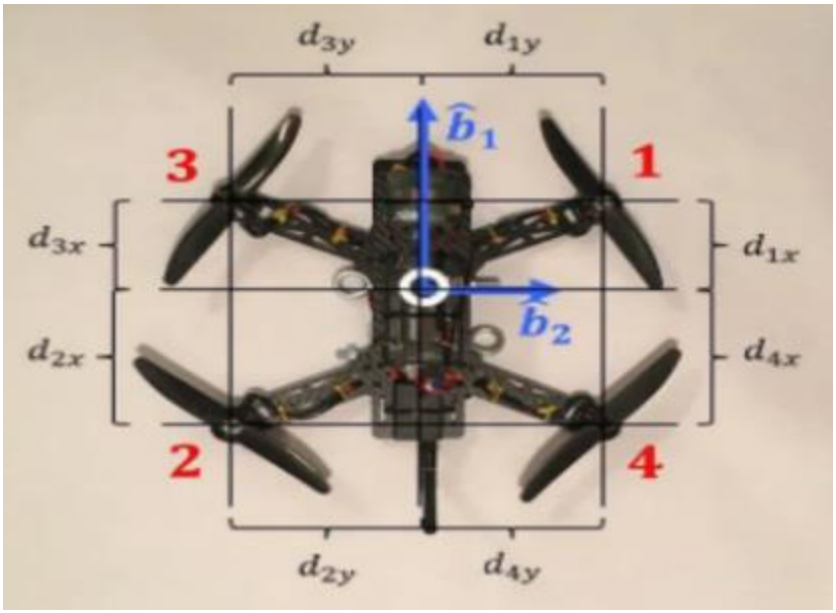

Figure 11 Propeller's Distance from Centre of Gravity (CG) (Tytler 2017b)

Following equation, 3.11 represent the thrust equation of the vehicle

$$\begin{bmatrix} Fx \\ Fy \\ Fz \end{bmatrix} = \begin{bmatrix} 0 \\ 0 \\ -F1 - F2 - F3 - F4 \end{bmatrix} \quad 3.11$$

Moments are the simple product of forces and distance from the center of gravity around all three axes of the body frame.

Equation 3.12 shows the moment along the x-axis of the vehicle.

$$L = F_1 d_{1y} + F_2 d_{2y} - F_3 d_{3y} + F_4 d_{4y} \quad 3.12$$

Equation 3.13 shows the moment along the z-axis of the vehicle.

$$M = -F_1 d_{1x} + F_2 d_{2x} - F_3 d_{3x} + F_4 d_{4x} \quad 3.13$$

Yaw is produced in quadcopter by the rotation of the propellers. Two propellers rotate clockwise and the other two rotate counter-clockwise to balance the yaw moment (Figure 3.5). Equation 3.14 shows how to calculate the yaw moment of the quadcopter.

$$N = -T(F_1 d_{1x} d_{1y}) + -T\left(F_2 d_{2x} d_{2y}\right) + T(F_3 d_{3x} d_{3y}) + T(F_4 d_{4x}\, d_{4y}) \quad 3.14$$

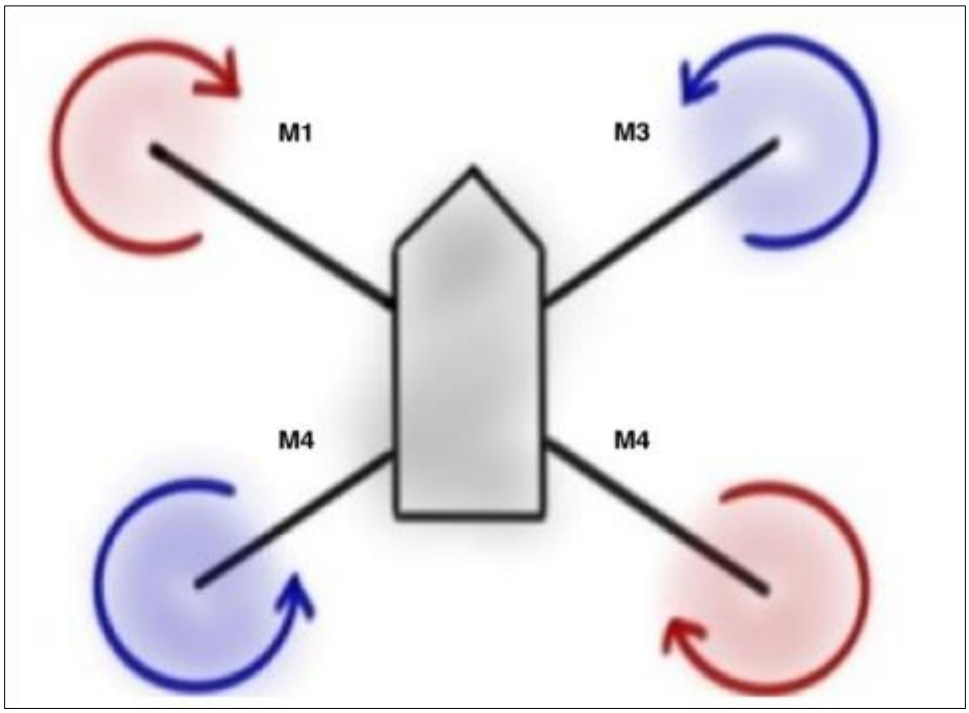

Figure 12 Motors Rotation Direction for Yaw Moment (Black Tie Aerial, 2014)

3.4.2. Gravity in Body Frame

The force of gravity acting on the vehicle can be represented in the body frame using Euler angles. Transformation matrix C_n^b from equation 3.2 can be used for this purpose. Where C_n^b is inertial to the body frame transformation matrix, F_g^n and F_g^b represents the force of gravity in inertial and body frames of references respectively. Equation 3.15 shows the force of gravity in an inertial frame of reference.

$$F_g^n = \begin{bmatrix} 0 \\ 0 \\ mg \end{bmatrix} \tag{3.15}$$

Equation 3.15 is multiplied with inertial to body frame transformation matrix C_n^b to get the force of gravity in the body frame of reference (Equation 3.16).

$$F_n^g = \begin{bmatrix} \cos(\theta)\cos(\psi) & \cos(\theta)\sin(\psi) & -\sin(\theta) \\ -\cos(\theta)\sin(\psi) + \cos(\psi)\sin(\varphi)\sin(\theta) & \cos(\psi)\cos(\varphi) + \sin(\theta)\sin(\varphi)\sin(\psi) & \text{coss}(\theta)\sin(\varphi) \\ \sin(\psi)\sin(\varphi) + \sin(\theta)\cos(\varphi)\sin(\psi) & -\sin(\varphi)\cos(\psi) + \sin(\theta)\cos(\varphi)\sin(\psi) & \text{coss}(\theta)\cos(\varphi) \end{bmatrix} \begin{bmatrix} 0 \\ 0 \\ mg \end{bmatrix} \tag{3.16}$$

After multiplication, equation 3.16 simplifies as equation 3.17.

$$F_g^n = \begin{bmatrix} -mgsin(\theta) \\ mgsin(\varphi)\cos(\theta) \\ mgcos(mgcos(\varphi)\cos(\theta)) \end{bmatrix} \tag{3.17}$$

3.4.3. Moments of Inertia

The moment of inertia, which is given in matrix form (Equation 3.18), provides the amount of time required to halt a rotating item and to rotate a still object. A moment was required around all three axes of the vehicle. The distance squared from the body's centre of mass equals the moment of inertia.

$$I = \begin{bmatrix} I_{xx} & -I_{xy} & -I_{xz} \\ -I_{yx} & I_{yy} & -I_{yz} \\ -\mathrm{I}_{xz} & -I_{yz} & I_{zz} \end{bmatrix} \tag{3.18}$$

The moment of inertia on opposing sides of the vehicle cancels each other out for a symmetrical body. Since I assumed that the vehicle is symmetrical, Equation 3.19 will simplify the inertia matrix. (Tytler, 2017b.)

$$I = \begin{bmatrix} I_{xx} & 0 & 0 \\ 0 & I_{yy} & 0 \\ 0 & 0 & I_{zz} \end{bmatrix} \quad 3.19$$

3.4.4. Linear Acceleration and Motion

Using Coriolis theorem, equation 3.6, we can convert inertial acceleration into a rotating body frame. Equation 3.20 shows the inertial acceleration conversion into body frame acceleration.

$$\dot{V}^b = \begin{bmatrix} \dot{u} \\ \dot{v} \\ \dot{w} \end{bmatrix}^b + \begin{bmatrix} 0 & -r & q \\ r & 0 & -p \\ -q & p & 0 \end{bmatrix} \begin{bmatrix} u \\ v \\ w \end{bmatrix}^b = \begin{bmatrix} \dot{u} + qw - rv \\ \dot{v} + ru - pw \\ \dot{w} + pv - qu \end{bmatrix} \quad 3.20$$

By substituting forces and acceleration in Newton's 2nd law F=ma we can get linear motion equations 3.21.

$$\begin{bmatrix} -mgsin(\theta) \\ mgsin(\varphi)\cos(\theta) \\ -F1 - F2 - F3 - F4mgcos(mgcos(\varphi)\cos(\theta)) \end{bmatrix} = m \begin{bmatrix} \dot{u} + qw - rv \\ \dot{v} + ru - pw \\ \dot{w} + pv - qu \end{bmatrix} \quad 3.21$$

3.4.5. Rotational Acceleration

Using Coriolis Theorem equation 3.6 again as above in equation 3.20, we can get rotational acceleration equation 3.22, the difference is that, here we use the angular instead of linear velocity.

$$\begin{bmatrix} L \\ M \\ N \end{bmatrix} = \begin{bmatrix} I_{xx} & 0 & 0 \\ 0 & I_{yy} & 0 \\ 0 & 0 & I_{zz} \end{bmatrix} \begin{bmatrix} \dot{p} \\ \dot{q} \\ \dot{q} \end{bmatrix}^b + \begin{bmatrix} 0 & -r & q \\ r & 0 & -p \\ -q & p & 0 \end{bmatrix} \begin{bmatrix} I_{xx} & 0 & 0 \\ 0 & I_{yy} & 0 \\ 0 & 0 & I_{zz} \end{bmatrix} \begin{bmatrix} p \\ q \\ r \end{bmatrix} \quad 3.22$$

After addition and multiplication, equation 3.22 simplifies as equation 3.23.

$$\begin{bmatrix} L \\ M \\ N \end{bmatrix} = \begin{bmatrix} \dot{p}Ixx \\ \dot{q}Iyy \\ \dot{q}Izz \end{bmatrix} + \begin{bmatrix} -I_{xx}qr + I_{zz}qr \\ I_{xx}pr - I_{zz}pr \\ -I_{xx}pq + I_{yy}pq \end{bmatrix} \quad 3.23$$

3.5. Angular Velocity and Euler Angles

We know, how the angular velocities p, q, and r, are changing over time and a gyro will give us these values, but these are not the same as Euler angles φ, θ and Ψ. Angular velocity is the rate of change of angles with the body axis, while Euler angles are rotation in their frame of reference. Using the coordinate transformation, angular velocity can be represented as the Euler angle derivative (Equation 3.24). (Tytler 2017b.)

$$\begin{bmatrix} p \\ q \\ r \end{bmatrix} = \begin{bmatrix} 1 & 0 & 0 \\ 0 & \cos(\varphi) & \sin(\varphi) \\ 0 & -\sin(\varphi) & \cos(\varphi) \end{bmatrix} \begin{bmatrix} \cos(\theta) & 0 & -\sin(\theta) \\ 0 & 1 & 0 \\ \sin(\theta) & 0 & \cos(\theta) \end{bmatrix} \begin{bmatrix} p \\ q \\ r \end{bmatrix} + \begin{bmatrix} 1 & 0 & 0 \\ 0 & \cos(\varphi) & \sin(\varphi) \\ 0 & -\sin(\varphi) & \cos(\varphi) \end{bmatrix} \begin{bmatrix} 0 \\ \dot{\theta} \\ 0 \end{bmatrix} + \begin{bmatrix} \varphi \\ 0 \\ 0 \end{bmatrix} \quad 3.24$$

Equation 3.24 simplifies as Equation 3.25.

$$\begin{bmatrix} p \\ q \\ r \end{bmatrix} = \begin{bmatrix} -\dot{\Psi}\sin(\theta) \\ \dot{\Psi}\cos(\theta)\sin(\varphi) \\ \dot{\Psi}\cos(\varphi)\cos(\theta) \end{bmatrix} + \begin{bmatrix} 0 \\ \dot{\theta}\cos(\varphi) \\ \dot{\theta}\sin(\varphi) \end{bmatrix} + \begin{bmatrix} \varphi \\ 0 \\ 0 \end{bmatrix} \quad 3.25$$

Finally, the equations look as follows

$$p = \dot{\varphi} + \dot{\Psi}\sin(\theta) \quad 3.26$$

$$q = \theta\dot{\cos}(\varphi) + \dot{\Psi}\sin(\theta)\sin(\varphi) \quad 3.27$$

$$r = \Psi\dot{\cos}(\varphi)\cos(\theta) + \dot{\theta}\sin(\varphi) \quad 3.28$$

3.6. Inertial Coordinate

To calculate the position of the vehicle in an inertial frame, we simply use the Euler angle transformation matrix C_n^b equation 3.3 to convert body frame velocities to an inertial coordinate position (Equation 3.29). Where $x^{\dot{E}}$, $y^{\dot{E}}$ and $z^{\dot{E}}$ represents the first derivative of the X, Y, and Z positions of the vehicle in an inertial frame. (Tytler 2017b.)

$$\begin{bmatrix} x^{\dot{E}} \\ y^{\dot{E}} \\ z^{\dot{E}} \end{bmatrix} = \begin{bmatrix} \cos(\theta)\cos(\psi) & -\cos(\theta)\sin(\psi) + \cos(\psi)\sin(\varphi)\sin(\theta) & \sin(\psi)\sin(\varphi) + \sin(\theta)\cos(\varphi)\cos(\psi) \\ \cos(\theta)\sin(\psi) & \cos(\psi)\cos(\varphi) + \sin(\theta)\sin(\varphi)\sin(\psi) & -\sin(\varphi)\cos(\psi) + \sin(\theta)\cos(\varphi)\sin(\psi) \\ -\sin(\theta) & \mathrm{coss}(\theta)\sin(\varphi) & \mathrm{coss}(\theta)\cos(\varphi) \end{bmatrix} \begin{bmatrix} u \\ v \\ w \end{bmatrix}^b \quad 3.29$$

3.7. Non-Linear Equations

By simple mathematical operations on the matrices above, we can rewrite the equations in non-linear form and can modify them as we want. Equations are represented below. (Tytler 2017b.)

$$\dot{u} = -gsin(\theta) + rv - qw \quad 3.30$$

$$\dot{v} = -gsin(\varphi)\cos(\theta) + ru + pw \quad 3.31$$

$$\dot{w} = \frac{1}{m}(-Fz) + gcos(\varphi)\cos(\theta) - qu - pv \quad 3.32$$

$$\dot{p} = \frac{1}{Ixx}(L + (Iyy - Izz)qr) \quad 3.33$$

$$\dot{p} = \frac{1}{Iyy}(M + (Izz - Ixx)pr) \quad 3.34$$

$$\dot{p} = \frac{1}{Izz}(N + (Ixx - Iyy)pr) \quad 3.35$$

$$\dot{\varphi} = (p + \big(qsin(\varphi) - rcos(\varphi)\big)\tan(\theta)) \quad 3.36$$

$$\dot{\varphi} = qcos(\varphi) - rsin(\varphi) \quad 3.37$$

$$\dot{\varphi} = \big(qsin(\varphi) - rcos(\varphi)\big)\sec(\theta) \quad 3.38$$

$$\dot{\varphi} = \big(qsin(\varphi) - rcos(\varphi)\big)\sec(\theta) \quad 3.39$$

Non-Linear equations represent the dynamic behavior of the quadcopter, but we still need to represent the equations including motors rpm, propellers thrust, the mass of the quadcopter, torque functions, and inertial variables values

4. Result

The UAV exhibited stable flight characteristics with controllable pitch, roll, and yaw movements. The flight controller effectively maintained altitude and stability under varying wind conditions. The average flight time was approximately 3 minutes as configured in the MATLAB R2023a code, allowing for extended surveillance missions.

The simulated security and surveillance UAV was equipped with the following specifications as shows in Table 4.1.

Table 6 Specifications of the Simulated UAV

Weight	1.25kg
Motor maximum tilt angle	35^0
Length	0.265m
Maximum roll angle	50^0
Ixx	0.0232m
Iyy	0.0232m
Izz	0.0468m
Maximum pitch angle	30^0
Maximum thrust	2.5kg
Maximum extra payload	1kg
Simulation time	3mins

The UAV's performance was simulated using a software tools, MATLAB/Simulink. The simulation involved various scenarios, including indoor and outdoor flights, obstacle avoidance, and GPS navigation.

5. Discussion

Using MATLAB R2023a visualization capabilities to create 3D animations or plots that shows the drone movement and orientation throughout the simulation. This provides a visual representation of how the drone responds to the control inputs and external disturbances, It is a powerful programming and numerical computing environment widely used in various scientific, engineering, and research disciplines for data analysis, simulation, and visualization. Plotting in MATLAB R2023a allows to convey complex data relationships, trends, and patterns through graphical representations, making it easier to interpret and analyze data.

The quadcopter adhering to real-world constraints is represented by the MATLAB R2023a model. Plotting is utilised for visualisation in MATLAB R2023a since it is more practical and efficient. Plotting of altitude, pitch, theta, and psine is done using several plotting methods to compare and track changes in behaviour. When every motor rotates at the same speed, the first thrust is produced. Figure 4.1 depicts the response of the vehicle. In MATLAB R2023a, a signal-builder block Figure 4.1 is used to plan a trajectory that shows the vehicle's performance when many signals are applied simultaneously. Because roll, pitch, and yaw are controlled in the body coordinate system rather than X, Y, and Z in the inertial coordinate system, the inertial trajectory is unpredictable. The following are several signal commands and the simulation's answers to them. The altitude instruction in the three-minute simulation is a ramp signal (Figure 4.1) with a slope of 1.

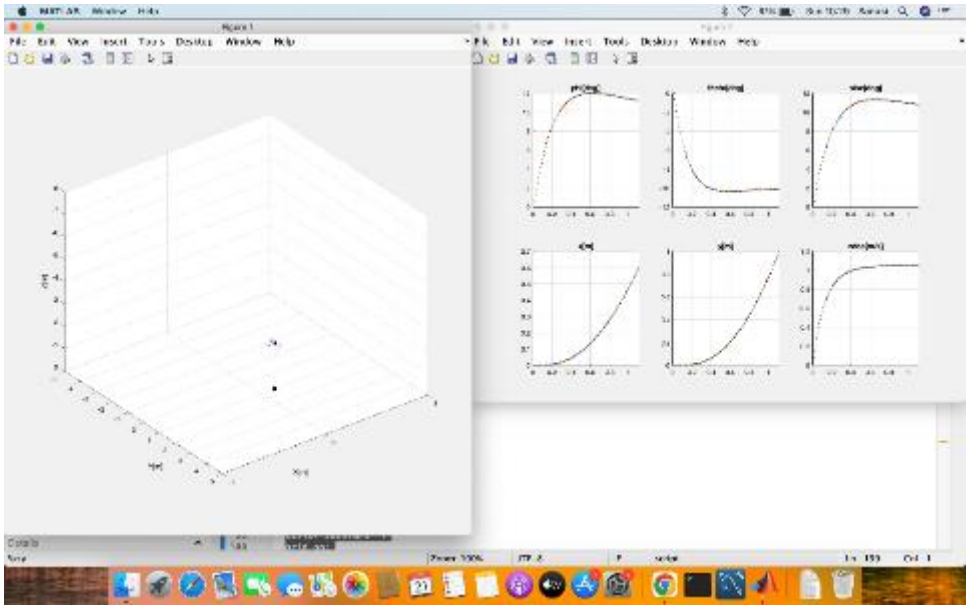

Figure 13 Quadcopter's 3D Trajectory and Simulation Response in Signal Form

Two individual plots shows in Figure 4.1 and this is as a result shows in Table 4.1, the plots indicate the quadcopter 3D trajectory and the 6 six of freedom simulation reponses. The 3D trajectory shows how the quadcopter navigate around. The trajectory commonly used to describe the full range of motion a drone can experience in a 3D space. MATLAB R2023a is a powerful tool that can be used to simulate the behavior of a drone using its built-in functionalities and toolboxes. Here's how you can simulate the six degrees of freedom of a drone using MATLAB R2023a

In the context of design and simulation for unmanned aerial vehicles (UAVs), the term six degrees of freedom (6DoF) refers to the six distinct ways in which an object can move in three-dimensional space. These degrees of freedom encompass the translational and rotational motions that characterize the movement and orientation of the UAV. Understanding and simulating these six degrees of freedom is essential for designing, analyzing, and controlling UAVs effectively.

Analyzing drone simulation using the six degrees of freedom (6DoF) framework involves understanding the fundamental ways in which a drone can move within its environment. The 6DoF model describes a drone's motion in terms of three translational degrees of freedom (movement in three orthogonal directions) and three rotational degrees of freedom (movement around three orthogonal axes).

Translational Degrees of Freedom: Translational degrees of freedom refer to the drone's ability to move in three different directions in space forward/backward (X-axis), left/right (Y-axis), and up/down (Z-axis). These movements are typically controlled using the drone's propulsion system, such as its motors and propellers. In a simulation, the accuracy of these movements can be assessed by evaluating how well the drone responds to control inputs and how closely its simulated position matches the expected position

Rotational Degrees of Freedom: Rotational degrees of freedom refer to the drone's ability to rotate around three different axes: roll, pitch, and yaw. Roll is the rotation around the longitudinal axis (front to back), pitch is the rotation around the lateral axis (side to side), and yaw is the rotation around the vertical axis (up and down). These rotations are controlled by adjusting the drone's motor speeds in a coordinated manner. In a simulation, evaluating the drone's rotational behavior involves observing how well it maintains its orientation and stability in response to control inputs.

Simulation Accuracy and Realism: A key aspect of analyzing a drone simulation is assessing its accuracy and realism. The simulation should accurately replicate the physics and dynamics of drone flight, taking into account factors like aerodynamics, motor behavior, sensor inputs, and environmental conditions (wind, turbulence, etc.). Accurate simulation is crucial for testing and validating control algorithms, sensor fusion algorithms, and other drone-related technologies before implementing them on a physical drone.

Control Algorithms and Responses: Drone simulations are valuable tools for testing and refining control algorithms. The simulation allows developers to assess how well a drone responds to various control inputs and maneuvers. For

instance, evaluating how the drone reacts to different PID (Proportional-Integral-Derivative) controller settings or trajectory tracking algorithms can provide insights into its stability, agility, and overall flight performance.

Sensor Simulation and Fusion: Many drones rely on various sensors such as accelerometers, gyroscopes, GPS, and cameras for navigation and control. Simulating these sensors and their interactions with the drone's control system is essential. Sensor simulation helps analyze how sensor measurements are affected by the drone's motion and external factors. Sensor fusion algorithms, which combine data from multiple sensors to obtain a more accurate estimation of the drone's state, can also be evaluated in a simulated environment.

Collision and Obstacle Avoidance: Simulating collision avoidance and obstacle detection algorithms is critical for ensuring the safety of drone operations. Drone simulations can replicate scenarios in which the drone encounters obstacles and assess how well its collision avoidance system functions. This analysis helps in fine-tuning the drone's behavior in complex environments and verifying its ability to navigate safely.

In summary, analyzing a drone simulation using the 6 degrees of freedom framework involves assessing the accuracy of translational and rotational movements, evaluating the realism of the simulation, testing and refining control algorithms, simulating sensor behavior and fusion, and validating collision avoidance strategies. These analyses collectively contribute to the development of safer, more capable, and more reliable drone systems for a wide range of applications.

6. Conclusion

This project represents a significant advancement in the field of modern security and surveillance technologies. Throughout the course of this endeavor, a comprehensive exploration of UAV design, system integration, and simulation techniques has been undertaken to create a robust and efficient aerial solution for monitoring and safeguarding various environments. The project began by delving into the fundamental aspects of UAV design, encompassing aerodynamics, propulsion, and structural considerations. By addressing these critical elements, I ensured the UAV's ability to achieve optimal flight performance, stability, and endurance, vital characteristics for its role in security and surveillance operations.

Simulation played a pivotal role in refining the UAV's operational efficiency and effectiveness. Through sophisticated simulation software, I meticulously validated the UAV's flight dynamics, sensor accuracy, and mission planning algorithms. This approach allowed for iterative optimization, reducing the risk of errors during real-world deployment and ensuring that the UAV performs flawlessly in various scenarios. The implications of this project are far-reaching. The security and surveillance UAV developed here can be instrumental in a myriad of applications, including border control, disaster response, wildlife monitoring, and critical infrastructure protection. Its ability to operate autonomously or under remote human supervision adds a layer of versatility that is essential in complex and dynamic environments.

In conclusion, the design and simulation of a security and surveillance UAV is a testament to the relentless pursuit of innovation in technology. This project showcases the potential for unmanned aerial vehicles to revolutionize the realm of security and surveillance, offering a reliable, adaptable, and efficient solution to safeguarding our increasingly complex and interconnected world. By amalgamating engineering acumen, cutting-edge sensors, and advanced simulation techniques, this project exemplifies the boundless possibilities that emerge at the intersection of aerial robotics and security.

Recommendation

Further research and development have the potential to enhance the functionality of this design, as unmanned aerial vehicles are increasingly becoming a valuable and intriguing area of research. Numerous advancements in design will need to be made in the future to maximize the effectiveness and usefulness of this design for the community. To enhance the responsiveness and utility of the UAV in the future, I suggest including the following features: integrating a solar panel to extend the UAV's flight duration and implementing autonomous transmission capabilities.

Compliance with ethical standards

Disclosure of conflict of interest

No conflict of interest to be disclosed.

References

[1] Abdel-Aziz, Y. I., Karara, H. M., & Hauck, M. (2015). Direct linear transformation from comparator coordinates into object space coordinates in close-range photogrammetry. *Photogrammetric engineering & remote sensing*, *81*(2), 103-107.

[2] Ahmed, A., Ngoduy, D., Adnan, M., & Baig, M. A. U. (2021). On the fundamental diagram and driving behavior modeling of heterogeneous traffic flow using UAV-based data. Transportation research part A: policy and practice, 148, 100-115.

[3] Akinnuli, B. O., Agboola, O. O., & Ikubanni, P. P. (2017). Design and development of an unmanned surveillance aerial vehicle (Usav) using locally sourced material. ANNALS of Faculty Engineering Hunedoara–International Journal of Engineering, 15(3), 27-32

[4] Alzahrani, B., Oubbati, O. S., Barnawi, A., Atiquzzaman, M., & Alghazzawi, D. (2020). UAV assistance paradigm: State-of-the-art in applications and challenges. Journal of Network and Computer Applications, 166, 102706.

[5] Basu, P., Redi, J., & Shurbanov, V. (2004, October). Coordinated flocking of UAVs for improved connectivity of mobile ground nodes. In *IEEE MILCOM 2004. Military Communications Conference, 2004.* (Vol. 3, pp. 1628-1634). IEEE

[6] Biomo, J. D. M. M., Kunz, T., & St-Hilaire, M. (2014, May). An enhanced Gauss-Markov mobility modelfor simulations of unmanned aerial ad hoc networks. In *2014 7th IFIP Wireless and Mobile Networking Conference (WMNC)* (pp. 1-8). IEEE.

[7] Black Tie Aerial (2014) The Physics of Quadcopter Flight. https://blacktieaerial.com/the-physics- of-quadcopter-flight/ Accessed in June 2019.

[8] Bouachir, O., Abrassart, A., Garcia, F., & Larrieu, N. (2014, May). A mobility model for UAV ad hoc network. In *2014 international conference on unmanned aircraft systems (ICUAS)* (pp. 383-388). IEEE.

[9] Brener, N. D., Kann, L., Shanklin, S., Kinchen, S., Eaton, D. K., Hawkins, J., & Flint, K. H. (2013). Methodology of the youth risk behavior surveillance system—2013. Morbidity and Mortality Weekly Report: Recommendations and Reports, 62(1), 1-20

[10] Briante, O., Loscri, V., Pace, P., Ruggeri, G., & Zema, N. R. (2015). Comvivor: an evolutionary communication framework based on survivors' devices reuse. *Wireless personal communications*, *85*, 2021-2040.

[11] Cox, T. H., Nagy, C. J., Skoog, M. A., Somers, I. A., & Warner, R. Civil UAV Capability Assessment.

[12] Colomina, I., & Molina, P. (2014). Unmanned aerial systems for photogrammetry and remote sensing: A review. ISPRS Journal of photogrammetry and remote sensing, 92, 79-97

[13] Demir, K., Cicibas, H., & Arica, N. (2015). Unmanned aerial vehicle domain: Areas of research. Defence science journal, 65(4)

[14] Deschênes, P. (2019). The Rise of the Drones: Technological Development of Miniaturised Weapons and the Challenges for the Royal Canadian Navy

[15] Elloumi, M., Dhaou, R., Escrig, B., Idoudi, H., & Saidane, L. A. (2018, April). Monitoring road traffic with a UAV-based system. In *2018 IEEE wireless communications and networking conference (WCNC)* (pp. 1-6). IEEE.

[16] Erman, A. T., van Hoesel, L., Havinga, P., & Wu, J. (2008). Enabling mobility in heterogeneous wireless sensor networks cooperating with UAVs for mission-critical management. *IEEE Wireless Communications*, *15*(6), 38-46.

[17] Etkin, B., & Reid, L. D. (1996). Mean Aerodynamic Chord, Mean Aerodynamic Center, and ac m C. Dynamics of Flight: Stability and Control, 3rd ed., Wiley, New York, NY, 357-363.

[18] Fernandez, S. G., Vijayakumar, K., Palanisamy, R., Selvakumar, K., Karthikeyan, D., Selvabharathi, D., ... & Kalyanasundhram, V. (2019). Unmanned and autonomous ground vehicle. International Journal of Electrical and Computer Engineering, 9(5), 4466.

[19] Hildmann, H., & Kovacs, E. (2019). Using unmanned aerial vehicles (UAVs) as mobile sensing platforms (MSPs) for disaster response, civil security and public safety. Drones, 3(3), 59.

[20] Hoffmann, G., Huang, H., Waslander, S., & Tomlin, C. (2007, August). Quadrotor helicopter flight dynamics and control: Theory and experiment. In *AIAA guidance, navigation and control conference and exhibit* (p. 6461).

[21] Hugenholtz, C. H., Moorman, B. J., Riddell, K., & Whitehead, K. (2012). Small unmanned aircraft systems for remote sensing and earth science research. *Eos, Transactions American Geophysical Union*, *93*(25), 236-236.

[22] Jain, S. K., Mohammad, S., Bora, S., & Singh, M. (2015). A review paper on: autonomous underwater vehicle. International Journal of Scientific & Engineering Research, 6(2), 38.

[23] Khan, A., Schaefer, D., Tao, L., Miller, D. J., Sun, K., Zondlo, M. A., ... & Lary, D. J. (2012). Low power greenhouse gas sensors for unmanned aerial vehicles. *Remote Sensing*, *4*(5), 1355- 1368.

[24] Kindervater, K. H. (2016). The emergence of lethal surveillance: Watching and killing in the history of drone technology. Security Dialogue, 47(3), 223-238.

[25] Kuiper, E., & Nadjm-Tehrani, S. (2006, July). Mobility models for UAV group reconnaissance applications. In *2006 International Conference on Wireless and Mobile Communications (ICWMC'06)* (pp. 33-33). IEEE.

[26] Menouar, H., Guvenc, I., Akkaya, K., Uluagac, A. S., Kadri, A., & Tuncer, A. (2017). UAV- enabled intelligent transportation systems for the smart city: Applications and challenges. *IEEE Communications Magazine*, *55*(3), 22-28

[27] Orfanus, D., & de Freitas, E. P. (2014, October). Comparison of UAV-based reconnaissance systems performance using realistic mobility models. In *2014 6th international congress on ultra modern telecommunications and control systems and workshops (ICUMT)* (pp. 248-253). IEEE.

[28] Oubbati, O. S., Atiquzzaman, M., Lorenz, P., Tareque, M. H., & Hossain, M. S. (2019). Routing in flying ad hoc networks: Survey, constraints, and future challenge perspectives. IEEE Access, 7, 81057-81105.

[29] Pawar, A. A., Nalbalwar, S. L., Deosarkar, S. B., & Singh, S. (2019). Surveillance Drone. International Research Journal of Engineering and Technology (IRJET), 6(07).

[30] Sadraey, M., & Müller, D. (2009). Drag force and drag coefficient. M. Sadraey, Aircraft Performance Analysis. VDM Verlag Dr. Müller.

[31] Sánchez-García, J., García-Campos, J. M., Toral, S. L., Reina, D. G., & Barrero, F. (2015, December). A self organising aerial ad hoc network mobility model for disaster scenarios. In *2015 international conference on developments of E-systems engineering (DeSE)* (pp. 35-40). IEEE.

[32] Shakhatreh, H., Sawalmeh, A. H., Al-Fuqaha, A., Dou, Z., Almaita, E., Khalil, I., ... & Guizani, M. (2019). Unmanned aerial vehicles (UAVs): A survey on civil applications and key research challenges. *Ieee Access*, *7*, 48572-48634.

[33] Stafford, J. (2014). *How a Quadcopter Works Clay Allen, University of Alaska, Fairbanks*. Retrieved 2015-01-20, Spring.

[34] Trilaksono, B. R., Nasution, S. H., & Purwanto, E. B. (2013, November). Design and implementation of hardware-in-the-loop-simulation for uav using pid control method. In 2013 3rd International Conference on Instrumentation, Communications, Information Technology and Biomedical Engineering (ICICI-BME) (pp. 124-130). IEEE.

[35] Tytler, C. (2017a) Modeling Vehicle Dynamics – Euler Angles. https://charlestytler.com/modeling-vehicle-dynamics-euler-angles/ Accessed in July 2019.

[36] Tytler, C. (2017b) Modeling Vehicle Dynamics – Quadcopter Equations ofMotion. https://charlestytler.com/quadcopter-equations-motion/ Accessed in July 2019.

[37] Wan, Y., Namuduri, K., Zhou, Y., & Fu, S. (2013). A smooth-turn mobility model for airborne networks. *IEEE Transactions on Vehicular Technology*, *62*(7), 3359-3370.

[38] Wang, W., Guan, X., Wang, B., & Wang, Y. (2010). A novel mobility model based on semi- random circular movement in mobile ad hoc networks. *Information Sciences*, *180*(3), 399- 413.

[39] Wikipedia (2019) Six degrees of freedom. https://en.wikipedia.org/wiki/Six_degrees_of_freedom Accessed in June 2019.

[40] Zhou, B., Xu, K., & Gerla, M. (2004, October). Group and swarm mobility models for ad hoc network scenarios using virtual tracks. In *IEEE MILCOM 2004. Military Communications Conference, 2004.* (Vol. 1, pp. 289-294). IEEE.

[41] Zhuo, X., Koch, T., Kurz, F., Fraundorfer, F., & Reinartz, P. (2017). Automatic UAV image geo- registration by matching UAV images to georeferenced image data. Remote Sensing, 9(4), 376